NASA TECHNICAL MEMORANDUM

NASA TM X-73,191

NASA TM X-73,191

NOTCHED AND UNNOTCHED FATIGUE BEHAVIOR OF ANGLE-PLY GRAPHITE/EPOXY COMPOSITES

S. V. Ramani and D. P. Williams

Ames Research Center
Moffett Field, Calif. 94035

December 1976

1. Report No.	2. Government Accession No.	3. Recipient's Catalog No.
NASA TM X-73,191		

4. Title and Subtitle	5. Report Date
NOTCHED AND UNNOTCHED FATIGUE BEHAVIOR OF ANGLE-PLY GRAPHITE/EPOXY COMPOSITES	6. Performing Organization Code

7. Author(s)	8. Performing Organization Report No.
S. V. Ramani and D. P. Williams	A-6862
	10. Work Unit No. 505-01-21-06-00-21
9. Performing Organization Name and Address: Ames Research Center, Moffett Field, Calif. 94035	11. Contract or Grant No.
	13. Type of Report and Period Covered: Technical Memorandum
12. Sponsoring Agency Name and Address: National Aeronautics and Space Administration, Washington, D. C. 20546	14. Sponsoring Agency Code

15. Supplementary Notes

16. Abstract

The axial fatigue behavior of both notched and unnotched graphite/epoxy composites has been studied as part of a continuing research investigation. In unnotched studies, conducted on a $[0/\pm30]_{3s}$ AS/3501 laminate, S-N ($\Delta\sigma$-log N_f) curves were determined for various stress ratios R using simply supported test specimens. Apparent fatigue limits (defined as stress amplitude at 5×10^6 cycles) in tension-tension (T-T) and compression-compression (C-C) cycling occurred at about 60% of the respective static strengths. The overall results were expressed in the form of a constant life diagram (i.e., Goodman Diagram) showing the relationship between mean stress and stress amplitude. The diagram illustrates a skew-symmetry in fatigue life caused by the relatively low compressive strength of the unrestrained test specimens used. In effect, a maximum in fatigue properties occurs at a positive value of mean stress. Results of this study are of significance in situations where structural members are buckling or crippling critical in design.

17. Key Words (Suggested by Author(s))
Graphite/epoxy composites
Angle-ply
Goodman Diagram
Notched fatigue

18. Distribution Statement
Unlimited

STAR Category - 24

19. Security Classif. (of this report)	20. Security Classif. (of this page)	21. No. of Pages	22. Price*
Unclassified	Unclassified	37	$3.75

*For sale by the National Technical Information Service, Springfield, Virginia 22161

NOTCHED AND UNNOTCHED FATIGUE BEHAVIOR OF ANGLE-PLY GRAPHITE/EPOXY COMPOSITES

S. V. Ramani[1] and D. P. Williams[1]

NASA-Ames Research Center

Moffett Field, Calif.

ABSTRACT: The axial fatigue behavior of both notched and unnotched graphite/epoxy composites has been studied as part of a continuing research investigation. In unnotched studies, conducted on a $[0/\pm30]_{3s}$ AS/3501 laminate, S-N ($\Delta\sigma$-log N_f) curves were determined for various stress ratios R using simply supported test specimens. Apparent fatigue limits (defined as stress amplitude at 5×10^6 cycles) in tension-tension (T-T) and compression-compression (C-C) cycling occurred at about 60% of the respective static strengths. The overall results were expressed in the form of a constant life diagram (i.e., Goodman Diagram) showing the relationship between mean stress and stress amplitude. The diagram illustrates a skew-symmetry in fatigue life caused by the relatively low compressive strength of the unrestrained test specimens used. In effect, a maximum in fatigue properties occurs at a positive value of mean stress. Results of this study are of significance in situations where structural members are buckling or crippling critical in design.

KEY WORDS: Composite materials, graphite/epoxy composites, angle-ply, residual strength, unnotched fatigue behavior, cyclic tests, damage accumulation, notched fatigue behavior, Goodman Diagram.

---

[1] Research Scientist and Chief, Materials and Physical Sciences Branch, respectively, NASA, Ames Research Center, Moffett Field, CA 94035.

In notched studies, fatigue damage accumulation in several AS/3501 and T300/934 laminates containing sharp notches and circular holes has been investigated. In T-T cycling ($R = 0, \sigma_{max}$ = 85% net strength), fatigue damage in the $[0/\pm\theta]_{3s}$ and $[0/\pm\theta/0]_{2s}$ (θ = 30°, 45°) laminates at 10^6 cycles was essentially confined to the region between axial splits at hole edges or between the specimen edge and notch root split for edge notches. Residual notch strength increased by as much as 40% at 2×10^6 cycles, while the corresponding increase in compliance was about 5%. No fatigue failure appeared possible at this stress level, which corresponded to 50% σ_u (σ_u is the unnotched strength). The results demonstrate the insensitivity of these laminates to T-T fatigue in the notched condition. At higher cyclic stress ranges (~70% σ_u) imposed on precycled specimens, fatigue failure could be induced through the general unnotched fatigue mechanisms operative in the net section. The $[0/\pm45/90]_{2s}$ laminate, in contrast, is susceptible to T-T fatigue failures at stress levels of the order of 50% of its σ_u, both in the notched and unnotched condition. Fatigue failure of this laminate occurred by a process of edge delamination. Under tension-compression (T-C) cycling for all laminates, fatigue damage propagated from the edge notches into the specimen interior and failure occurred when a critical amount of damage had built up ahead of a notch root. The rate of accumulation of fatigue damage in T-C fatigue could be described by measuring changes in the crack-opening displacement range (ΔCOD) during cycling.

National interest in achieving aircraft fuel conservation has resulted in a growing need for energy-efficient aircraft in both commercial air transportation and military aviation. This need calls for the use of advanced composites in both primary aircraft structures such as wings, fuselage and fins and in energy-efficient engine components such as fan blades, nacelle, and engine frames. The structural integrity of aircraft components is normally ensured by designing them to be damage tolerant under the static and cyclic loads they would encounter in service. They must be fail-safe, i.e., retain residual strength sufficient to withstand specified damage and load levels. While fail-safe concepts are well-developed for metal structures, they have been hard to come by for composite structures, due mainly to the complex mechanical behavior exhibited by these materials. This need has necessitated research in diverse areas including failure mode prediction, damage growth kinetics and life-prediction methodology. The present work is one step in this process. It examines the performance of several multidirectional graphite/epoxy laminates subjected to fatigue, from the standpoint of damage initiation, damage accumulation, changes in residual strength and compliance with cycling, flaw growth rates and modes of failure.

The paper initially summarizes the unnotched fatigue behavior of a typical angle-ply laminate $[0/\pm30]_{3s}$. The results of this study form the basis for examining notched fatigue behavior of similar laminates: $[0/\pm\theta]_{3s}$ and $[0/\pm\theta/0]_{2s}$ (θ = 30°, 45°). The mechanics of failure in fatigue of a quasi-isotropic laminate $[0/\pm45/90]_{2s}$ are also studied for comparison. The interrelationship between notched and unnotched fatigue behavior for these laminates under T-T cycling is discussed. Finally, damage accumulation in notched laminates subjected to T-C cycling is explored.

Experimental

The angle-ply laminates used in this investigation were manufactured by the Lockheed Missiles and Space Company from prepregnated tapes of Hercules AS/3501 (AS) and Fiberite T300/934 (T) systems. The layups used for the various laminates were as follows: $[0/\pm\theta]_{3s}$ (AS); and $[0/\pm\theta/0]_{2s}$ (AS&T), (θ = 30°, 45°); and $[0/\pm45/90]_{2s}$ (T). The fibers used in the tapes were of the high-strength (3200 MN/m^2), intermediate modulus (220 GN/m^2) variety. Consolidation of the layups was effected in an autoclave at a pressure of 0.7 MN/m^2 and a temperature of 350°F for 2 hr. The resultant sheets, with midplane symmetry, had a fiber content of about 0.63 V_f, a density of 1600 kg/m^3 and a thickness of about 2.5 mm. Parallel-sided coupons provided with fiberglass end tabs were machined from rectangular sections of tabbed laminates for use in all aspects of the test program. The length of the untabbed gage section was 37 mm and the overall specimen length was 150 mm. The unnotched fatigue studies were carried out using 9.5-mm-wide specimens, while the notched fatigue studies were performed on 25-mm- and 50-mm-wide plate specimens. Two notch configurations were used — symmetrical double-edge notches (DEN) and center circular holes (CCN). Notch roots of edge notches were sharpened with a slitting saw to provide a root diameter of 0.125 mm.

Static and cyclic tests were conducted in an MTS closed loop, servo-hydraulic test system using hydraulic grips. A 25-mm gage length extensometer was used to measure strains in both static and unnotched fatigue tests. The knife edges of the extensometer were modified for use with 25-mm-wide notched specimens in tests involving compliance measurements. In T-C fatigue tests on 25-mm- and 50-mm-wide edge-notched specimens, crack-opening displacement (COD) was continuously monitored using a data

acquisition system. The COD gage was clipped to the knife edges, which were either bonded on to the specimen edges or clamped on to the specimen faces by means of screws located in the region near the edges. The specimen faces were vapor-deposited with a thin layer of aluminum and, further, superposed with a fine gold grid in an effort to measure transverse crack extension, if it should occur in cyclic tests. The coating was also expected to aid observations of surface damage during the course of a test. Notched specimens were also subjected to X-ray analysis after a given history of cycling in order to study the initiation and propagation of damage from notches and holes and to identify failure modes and mechanisms. Tetrabromoethane (TBE) opaque additive was used on the fatigue-damaged specimens prior to X-ray radiography to obtain sharp images of fine scale damage [1], e.g., failure within a 90° ply.

In compression tests, as well as in fatigue tests involving compressive loads, the tabbed specimens were not provided with face or edge supports to restrain them from buckling or grossly delaminating under strong compressive stresses. In other words, test specimens were simply supported. However, care was taken to ensure that compressive loads used in T-C fatigue tests were generally within the limit of linearity of stress-strain behavior in compression for unnotched specimens and within the straight section of the load-COD curve in compression for the notched specimens.

Results

Static Strengths

The static strengths of the laminates studied are listed in Table 1. The $[0/\pm\theta/0]_{2s}$ (θ = 30°, 45°) AS laminates exhibit a large scatter in

strength in the unnotched condition. In contrast, the T300/934 laminates exhibit scatter within 5% of the average unnotched strength value. A strong notch sensitivity is displayed by all laminates considered, the extent of which is greater for the relatively strongly anisotropic $[0/\pm\theta/0]_{2s}$ type than for the quasi-isotropic $[0/\pm45/90]_{2s}$ laminate. The strength in compression σ_c is an apparent value, since specimens were not provided with face or edge supports in compression tests. The same value of apparent σ_c, measured on 50-mm-wide DEN specimens for all laminates, indicates that the reported values for σ_c are a consequence of instability arising from specimen geometry alone. The criterion for the selection of loads in T-C fatigue tests was, therefore, based on the limit of linearity of the load-COD curve in a compression test (as noted in the preceding section), which occurred at a value of 70% of the apparent σ_c.

Unnotched Fatigue of $[0/\pm30]_{3s}$ *AS Laminate*

Detailed results of this study, including overall fatigue behavior, modulus degradation under cyclic loading, hysteresis loop changes in T-C fatigue and failure modes and mechanisms are given in ref. [2]. However, the main results are summarized here to project a general idea of unnotched fatigue behavior of angle-ply laminates and for later comparison with T-T notched fatigue behavior.

S-N curves for T-T (R = 0.1) and C-C (R = 10) cycling are given in Fig. 1. Static scatter range for both tension and compression are shown at N = 1. The lowered strength in compression (0.54 tensile strength) is due to the unrestrained test specimens used. The S-N curves lie well below the respective static scatterbands, demonstrating the existence of a real

fatigue effect. Fatigue limits (defined as stress amplitude at 5×10^6 cycles) occur at about 60% of the respective static strengths. The effect of a combination of tensile and compressive stresses on fatigue behavior was studied by generating stress-life data for a range of negative R values. The overall fatigue results are summarized in Fig. 2 in the form of a Goodman Diagram. In this figure, stress amplitude is plotted against the mean stress for various values of constant life; superimposed are straight lines representing a range of R values. The diagram exhibits a skew-symmetry in fatigue properties arising from the low compressive strength of the test specimens used. As a result, a maximum in fatigue properties occurs at a positive value of mean stress.

Subsequent to the fatigue investigations, compression tests were performed on fully face-supported and Celanese-type specimens. The results of these tests revealed that the true strength in compression for this laminate equals 80% of the strength in tension σ_u. This somewhat lower σ_c (compared with σ_u) is attributable to the failure mode in compression, which is total shear in a +30° or a -30° direction.

Notched T-T Fatigue Behavior of Angle-ply Laminates

The primary objectives of these studies were to characterize damage accumulation around sharp notches and circular holes in angle-ply laminates subjected to tension cycling (R = 0) and to identify conditions under which specimen failure would occur. The accumulation of fatigue damage was studied by determining the residual strength σ_r, change in compliance, and X-ray damage profile of specimens cycled at a stress range equal to 85% net strength for 10^3, 10^4, 10^5, 10^6 cycles and greater. Results of these studies are discussed in the following sections.

Fatigue Damage Accumulation in Notched $[0/\pm\theta]_{3s}$ *and* $[0/\pm\theta/0]_{2s}$ *(θ = 30°, 45°) Laminates* — The general behavior of this class of laminates containing only 0° and ±θ° plies is similar, and is typified by the performance of the $[0/\pm45/0]_{2s}$ T laminate with center circular notch which is discussed here. The residual strength and compliance of this laminate progressively increased with cycling as shown in Fig. 3. A 40% increase in residual strength over the static net section strength was observed at 2×10^6 cycles, while the corresponding increase in compliance was about 5%. The increase in σ_r is related to the progressive removal of the stress concentration effect of the hole through axial splitting at the hole edges. No fatigue failure was observed even after 5×10^6 cycles at this stress level, which corresponded to about 50% of the unnotched strength. The initiation and growth of damage around the hole may be described with reference to the sequence of X-ray radiographs shown in Fig. 4. At 10^3 cycles a zone of damage occurs around the hole, consisting of parallel vertical splits at the hole edges and some fine localized failure along 45° directions. With further cycling, the splits propagate vertically (notch root blunting effect) and failure in 45° directions originating at the hole boundary intensify. The diffuse zone of damage around the hole exhibits a strong tendency to spread predominantly in the stress direction. At 10^5 cycles, fine delamination between 0°, +45°, and -45° plies is evidenced in the edge view. Fatigue damage at 10^6 cycles is essentially confined to the region between splits, which at this stage have extended all the way into the grip section. Patches of delamination damage exist in the region bounded by the parallel splits and failure along 45° directions is mainly confined to this zone. Transverse spread of damage from the hole is very slight, if any. The edge view at 10^6 cycles discloses several sets of fine delamination cracks,

extending part way above and below the specimen midsection. These cracks suggest interlaminar weakening in T-T fatigue of the $[0/\pm45/0]_{2s}$ laminate and consequent potential degradation in compressive, transverse, and shear properties at long lives. It is not clear whether the observed fine scale delamination is a result of edge effects. The results, together with X-ray evidence of damage growth from the hole, however, suggest the relative insensitivity of these laminates to T-T fatigue in the notched condition.

In an effort to induce fatigue failure, notched, precycled specimens (with effectively increased strength) were cycled at higher cyclic stress ranges, in a separate series of experiments. When specimens were cycled at a $\Delta\sigma = 65\%\ \sigma_u$ for 1.5×10^6 cycles, σ_r increased to the unnotched net-section strength value, and no change in compliance was indicated. However, the postfatigue static fracture surface displayed a strong brooming effect, characteristic of interlaminar weakening, noted earlier. When notched specimens were cycled at even higher cyclic stress amplitudes ($\Delta\sigma$) (e.g., 70% σ_u and above), notable increase in specimen compliance occurred after several million cycles and the X-ray radiographs exhibited general failure along ±45° directions encompassing the entire gage section as shown in Fig. 5. These observations indicate that fatigue failure of the specimen would eventually occur through general unnotched failure mechanisms operating in the net section. Further, it is significant that even at these high values of $\Delta\sigma$, intense fatigue damage is contained in the vertical band bounded by the splits at hole edges. Therefore, it would appear that the notch itself plays only a negligible role in effecting transverse failure of these laminates.

When specimens containing symmetrical DEN were cycled in a similar manner ($R = 0$, σ_{max} = 85% net strength), axial splitting at notch roots

resulted and fatigue damage was contained between the specimen edge and the notch root split. In effect, the net section remained virtually undamaged. The residual net-section strength increased by 30% after 10^6 cycles with no attendant change in compliance. This implies a relative insensitivity to T-T fatigue in the notched state. The results of successively cycling a $[0/\pm45/0]_{2s}$ AS DEN specimen at increasingly higher $\Delta\sigma$ is schematically shown in Fig. 6. The value R_1 represents the residual net-section strength after initial cycling at 85% of the notched strength for 1.5×10^6 cycles. Subsequent cycling of the same specimen at 85% of R_1 for 1.5×10^6 cycles results in a residual strength equal to R_2 and on further cycling at 85% of R_2 for 1.5×10^6 cycles, σ_r increases to R_3, and so on. While the initial increase in σ_r is large (~30%), subsequent increases are smaller, being about 10 to 15% at each stage, i.e., $R_2 - R_1 = 10\%$, etc., demonstrating that significant notch root blunting occurs during the initial period of cycling. Eventually, a stress level is reached, where unnotched fatigue in the specimen net section occurs with attendant strong changes in specimen compliance (30 to 35%), which results in fatigue failure. The final σ_r value was found to be about 80% of the unnotched strength. These results of tension cycling DEN specimens are essentially identical to what was observed for the CCN specimens with the possible exception that σ_r for DEN specimens did not reach the unnotched strength level. This implies that the stress concentration effect of sharp notches is not completely removed through cyclic loading whereas it was for the case of holes. However, independent of notch geometry, final failure of notched specimens in T-T fatigue occurs at approximately 70% of unnotched strength for the $[0/\pm45/0]_{2s}$ laminates considered.

Fatigue Damage Accumulation in Notched $[0/\pm 45/90]_{2s}$ *Laminate* — Changes in residual strength and compliance with progressive cycling for specimens containing central holes are shown in Fig. 7. The corresponding X-ray record of damage at each stage is reproduced in Fig. 8. The residual strength initially increased, attaining a 15% increase over the original net section strength at 10^5 cycles but thereafter decreased sharply. Concomitant increase in specimen compliance was about 20% at 10^6 cycles, indicative of impending failure. Fatigue failure occurred at ~2×10^6 cycles at this stress level, which corresponds to 60% of the unnotched strength. The increase in σ_r up to 10^5 cycles is related to splitting or matrix shearing at the hole edges, with resultant partial blunting of the notch. This effect is noticeable from the X-ray pictures as early as 10^3 cycles, when a zone of damage, mainly in the form of vertical splits, develops around the hole. Some fiber-matrix separation along 45° directions occurs within the region bounded by the splits, and several 90° ply failures also occur, and these extend across the width of the specimen. These 90° failures are first observed in the lamina located in the midthickness of the specimen. At 10^4 cycles, the notch root splits are more pronounced and the extent of failure along 90° directions is noticeably increased. In the central region of the specimen, numerous closely spaced 90° failure lines can be observed and further, edge delamination between plies close to the specimen surface is apparent in the edge view. The damage around the hole is seen to have spread vertically to a considerable extent at 10^5 cycles. Failure along 45° directions intensifies, extending outwards into the specimen net section from the hole boundary. A further increase in density of failure in 90° plies is evident (also involving

outer 90° plies) and zones of delamination around the hole can be perceived. Beyond 10^5 cycles, however, the edge delamination effect becomes dominant, and is identified as the principal cause of eventual fatigue failure of the laminate. The X-ray picture at 10^6 cycles illustrates the propagation of edge delaminations from the specimen edges into the interior, with a resultant sharp decrease in σ_r (Fig. 7). Edge view reveals severe delamination between plies and kinks in delamination cracks, which are of two types — normal and oblique. The normal kink may be related to a delamination crack between a 0°/90° ply changing over to one between a 90°/-45° ply, while the oblique kink could occur when a delamination crack between a 90°/-45° ply changes over to become one between a +45°/-45° ply. Thus, delamination cracks appear to switch from between one set of plies to another set of plies via a cracked 45° or 90° ply. Eventually, the edge delaminations traverse the entire specimen width to effect failure. The apparent mechanism of failure suggests that the role of a notch in effecting fatigue failure is, at most, only secondary.

It is instructive to note that unnotched fatigue of this laminate occurred at the same $\Delta\sigma$ (60% σ_u) at which fatigue of notched specimens occurred. The mechanism of failure was identical, namely, edge delamination progressing across from specimen edges. In these tests, σ_r gradually decreased with accompanying loss in specimen stiffness, resulting in final failure. Further, tests on 50-mm-wide notched (6.5-mm-diameter hole) specimens have revealed that at a $\Delta\sigma$ equal to 40% σ_u, specimens can endure 5×10^6 cycles, although fine delamination cracks between plies occur. Such cracks signify potential degradation in properties with further cycling. Therefore,

it appears that the $[0/\pm45/90]_{2s}$ laminate is subject to fatigue damage even at relatively low stress levels, when free edge stresses are present.

Fatigue Damage Accumulation Under T-C Loading

In this part of the program, the accumulation of fatigue damage in edge-notched laminates subjected to T-C cycling has been investigated. Damage accumulation was monitored through continuous COD measurements during test. Surface observations of specimens were made with a low-power telescope as cycling progressed. Representative specimens were removed from the test machine very near failure (detected from COD readout) and examined by X-ray to determine failure mechanisms. As already noted in the Experimental Section, compressive stresses used were in the linear region of the load (P)-COD curves. Tests were conducted on both 25-mm- and 50-mm-wide DEN specimens of various laminates. The results of these studies are considered in the following sections.

T-C Cycling of $[0/\pm30]_{3s}$ *Laminate* — A typical Δ(COD) versus number of cycles plot for this laminate is shown in Fig. 9. The rate of accumulation of fatigue damage (defined as $d(\Delta COD)/dn$) can be described by two distinct stages as shown in Fig. 10. The first stage, characterized by a linear ΔCOD-N relation and relatively low damage growth rates, occupies the major proportion of specimen life. The second stage, in which ΔCOD increases exponentially with N, represents the terminal events leading to specimen failure. In Fig. 10, damage growth curves for three stress ranges denoted $\Delta\sigma_1$, $\Delta\sigma_2$ and $\Delta\sigma_3$ are shown and the corresponding $d(\Delta COD)/dN$ values are given in Table 2. The rates of damage accumulation in stages I and II increase as would be expected with increasing cyclic stress range. Of

interest, however, is the observation that final failure of the specimen in each case commences at a nearly constant value of ΔCOD, independent of the applied $\Delta\sigma$. This implies that a critical amount of damage builds up ahead of the notch root before failure occurs.

T-C Cycling of $[0/\pm\theta/0]_{2s}$ *(θ = 30°, 45°) and* $[0/\pm45/90]_{2s}$ *Laminates* — Similar damage accumulation tests under T-C cycling were carried out on $[0/\pm\theta/0]_{2s}$ (θ = 30°, 45°) laminates and the $[0/\pm45/90]_{2s}$ laminate. The results of these studies are summarized in Table 3. The fraction of life spent in stage I (linear ΔCOD-N region) is seen to be large in every case. The runout specimens correspond to cases where the compressive component in the stress range was equal to 60% of the apparent σ_c. In such cases, damage, though initiated at the notch roots, does not show an inclination to propagate. Only when compressive components were in the vicinity of 70% of apparent σ_c, did damage propagation occur. Referring to Table 3, it is seen that the $[0/\pm45/0]_{2s}$ T300/934 laminate exhibits a much stronger resistance to damage propagation than the corresponding $[0/\pm45/0]_{2s}$ AS/3501 (or the $[0/\pm30/0]_{2s}$ AS) laminate, despite the larger $\Delta\sigma$ applied for the former. It may be recalled that the $[0/\pm\theta/0]_{2s}$ AS laminates also exhibited large scatter in static properties, signifying generally poor quality of these laminates. The $[0/\pm45/90]_{2s}$ laminate, in comparison with the $[0/\pm\theta/0]_{2s}$ laminates, exhibits expectedly poor resistance to damage accumulation under T-C cycling, in view of the presence of 25% of 90° plies in this laminate.

For the various laminates examined, the nature of damage growth under T-C fatigue proceeded in a similar manner. Figure 11 illustrates damage in a specimen approaching failure. The vertical lines seen on the surface are measurement grids that were imprinted to track damage growth. However, the complexity of the observed cracking did not permit meaningful measurements to be made. The figure shows that a critical amount of damage accumulates in front of the notch roots before final failure occurs. Damage initiated in the form of splits at the notch roots fairly early in life. Surface observations indicated that the splits propagate into the net section, as cycling progressed, with resultant formation of multiple splits ahead of either notch. Eventually, a critical stage was reached, marked by rapid increases in ΔCOD as a function of cycles, and soon failure occurred in the compression stroke. It was also observed from hysteresis loops that the degradation in compressive stiffness of the specimens was much larger than the corresponding degradation in tensile stiffness measured in the concluding stages of these tests. Thus, failure appears to be governed by a loss in compressive properties of the specimen. X-ray radiographs revealed damage in the form of splitting, strong delaminations and intense failure in the $\pm\theta$ directions. The severity of damage precluded failure analysis on a local scale.

Discussion

Unnotched fatigue investigations on the $[0/\pm30]_{3s}$ laminate indicate that this laminate is subject to axial fatigue failures over a wide range of stress ratios, both positive and negative. Fatigue failures occur at stress levels that are 40% lower than the average static strengths, implying that a significant fatigue effect exists for this angle-ply laminate.

This behavior is in sharp contrast to the essentially fatigue-insensitive behavior exhibited by unidirectional graphite/epoxy at relatively high stress levels [3]. The present results, however, are in agreement with the work of Ryder [4] and demonstrate the occurrence of T-T fatigue failures in $[0/\pm45/90]_{2s}$ graphite/epoxy at stress levels at about 60% of the average static strength. It appears, therefore, that angle-ply graphite/epoxy composites are, in general, susceptible to tensile fatigue failures. The existence of a real fatigue limit for the $[0/\pm30]_{3s}$ laminate has not been verified; however, an apparent fatigue limit is indicated at about 60% of the static strength in T-T fatigue.

The fatigue results for the simply supported specimens of this study (Fig. 2) demonstrate that the maximum stress amplitude for 10^7 cycles life is 269 MN/m^2, the corresponding mean stress being 159 MN/m^2 and stress ratio being -0.2. Moreover, the constant life relationship is described by triangular-shaped curves (Fig. 2). The skew-symmetry in the constant life diagram results in fatigue properties that are poor in the mean stress region of 159 MN/m^2 to 0 MN/m^2 and worse for negative mean stresses. This is a consequence of the lowered strength in compression for the specimens and technique employed. In fully face-supported and Celanese-type specimens one might expect the maximum stress amplitude in fatigue to occur at a small positive mean stress, rather than at a fairly large value as observed in the present studies. This would have the effect of shifting the maximum properties close to the vertical line representing R = -1. Consequently, compressive components will not have an unexpectedly large influence on fatigue life as compared with tensile components. Nevertheless, the simple triangular shape of the Goodman Diagram as observed in the present work is different from the parabolic shape normally observed for metals as well as observed by Ryder

for the $[0/\pm45/90]_{2s}$ laminate. The exact implications of the differences in form of the Goodman Diagram, noted above, are, however, not clear.

While only limited unnotched fatigue testing was conducted on other laminates it appears that the apparent fatigue limit in T-T for the $[0/\pm\theta/0]_{2s}$ type laminates is closer to 70% of static ultimate strength, and for the $[0/\pm45/90]_{2s}$ laminate is less than 50% of its σ_u. Therefore, it would seem that the fatigue limit of graphite/epoxy laminates (in terms of respective percent static ultimate strength) increases with increasing percentage of 0° plies in the laminate. The unnotched fatigue mechanism in the $[0/\pm\theta/0]_{2s}$ laminates appears to be one of general failure along $\pm\theta°$ directions (as revealed by damage in the net section in the X-ray radiograph of Fig. 5) leading to failure of 0° plies in later stages when load is transferred to them by the failed $\pm\theta°$ plies. The dominant unnotched and notched fatigue failure mechanism for the $[0/\pm45/90]_{2s}$ laminate is edge delamination propagating across the specimen to effect failure.

With regard to the failure of laminates containing 90° plies, it has been shown analytically [5,6] and experimentally [7] that composite laminates with certain stacking sequences exhibit a tendency to delaminate at the edges under static and cyclic loading conditions. The $[0/\pm45/90]_s$ family of laminates is strongly susceptible to free-edge effects when stacking sequences of the form $[\pm45/90/0]_s$ and $[\pm45/0/90]_s$ occur and moderately susceptible when stacking follows the sequence $[0/\pm45/90]_s$. The theory proposed to explain this effect (5) suggests that for a given applied stress in the loading y direction, stresses generated in the x-direction induce a bending moment in the specimen. To counteract this bending moment, through-the-thickness z-stresses are called into play. The sign of the z-stresses is

dependent on the sign of the bending moment, which could be positive or negative depending on the laminate stacking sequence. The experimental observations in the present study are generally consistent with the delamination predictions; however, the extent of delamination under cyclic loading appears to be far more severe than the predictions for the simple static loading case. In this context, the X-ray study has established beyond doubt that failure of the $[0/\pm45/90]_{2s}$ laminate in T-T fatigue is governed by the occurrence of extensive edge delamination (Fig. 8). In the case of center notched laminates (CCN), damage around the hole spreads vertically rather than laterally with cycling and therefore, the hole does not appear to play any significant role in effecting fatigue failure. This conjecture is corroborated by the fact that unnotched specimens when cycled at the same $\Delta\sigma$ as the notched ones undergo fatigue failure through the same edge delamination mechanism. The hole thus plays a passive role in the mechanics of fatigue failure of the $[0/\pm45/90]_{2s}$ laminate under T-T cycling conditions. However, in the absence of free edge effects, the vertical spread of damage from a hole may constitute a significant mode of failure.

The failure of notched $[0/\pm\theta/0]_{2s}$ laminates in T-T fatigue is governed by the strong anisotropy introduced by the presence of 50% of 0° plies. The high ratio of longitudinal to transverse strength of the 0° lamina encourages splitting at notch roots in 0° plies. It is significant that fatigue damage is well contained between the parallel splits at hole edges (Fig. 4) and therefore, longitudinal propagation of damage (parallel to loading direction) constitutes an important mode of failure in situations where stresses act predominantly in the fiber direction. The small, but finite, amount of transverse cracking in $\pm\theta$° directions observed around

stress concentrators (Fig. 4) in the notched fatigue tests (σ_{max} = 50% σ_u) could be a factor of importance at long lives, e.g., 10^9 cycles. Moreover, the occurrence of fine edge delamination cracks in this layup (Fig. 4) is likely to affect compressive, shear, and transverse properties, particularly in the presence of a hostile environment (moisture, temperature). Further, the fact that edge effects occur under cyclic tensile loading in fiber-dominated laminates (50% or greater 0° plies) not containing 90° plies demonstrates that analytical predictions of edge delamination criteria in static loading do not directly apply to the occurrence of this phenomenon under cyclic loading. The results of the present studies, in general, indicate that one must be wary of using laminates prone to edge delamination problems, particularly under cyclic loading. Also, a need exists for predicting stacking sequences that will not delaminate in fatigue, specifically for laminates that do not contain 90° plies.

The experimental results demonstrate that it is possible to relate notched fatigue behavior to unnotched fatigue behavior for the various laminates under T-T cycling. For the $[0/\pm45/90]_{2s}$ laminate, the notched and unnotched fatigue behavior are virtually the same, since, in either case, failure occurs by edge delamination. In case of the notched (CCN) $[0/\pm\theta/0]_{2s}$ laminates, the notched situation reduces to unnotched fatigue behavior, since σ_r can be raised to the unnotched strength level, with resultant notch insensitivity. However, as already pointed out, the vertical zone of damage occurring in the stress direction in the $[0/\pm\theta/0]_{2s}$ laminates containing circular holes is a potential mode of failure in a real situation, e.g., a fastener hole in a bolted joint.

Under T-C cycling, the mode of damage growth and failure of notched laminates is significantly different from that observed for the T-T case. Fatigue damage at notch roots propagates in a progressive manner, thus enabling damage propagation to be semiquantitatively defined, such as through a COD concept. Results obtained indicate that monitoring of Δ(COD) during T-C cycling is a useful technique for comparing the resistance to damage accumulation in various laminates cycled under the same conditions.

Conclusions

1. The T-T unnotched fatigue limit (defined as endurance limit for 5×10^6 cycles) is about 60% of the static ultimate strength for the $[0/\pm30]_{3s}$ laminate, less than 50% for the $[0/\pm45/90]_{2s}$ laminate and closer to 70% for the $[0/\pm45/0]_{2s}$ laminate.
2. Goodman Diagram for the $[0/\pm30]_{3s}$ laminate, taking into consideration the true compressive strength of the laminate, demonstrates that compressive components in the stress range do not have an unexpectedly large influence over fatigue life as compared with tensile components.
3. The $[0/\pm\theta]_{3s}$ and $[0/\pm\theta/0]_{2s}$ laminates demonstrate relative insensitivity to T-T fatigue in the notched condition. The $[0/\pm45/90]_{2s}$ laminate, on the other hand, is susceptible to T-T fatigue failures in both the notched and unnotched conditions at relatively low stress levels through edge delamination effects.
4. Damage propagation from notches and holes in T-T fatigue occurs almost exclusively along the vertical (stress) direction. Damage is well-contained between axial splits at hole edges or between specimen edge and notch root split for edge notches. Transverse spread of damage from notches and holes is very slight even at stress levels where general unnotched fatigue in the specimen net section occurs.

5. Progressive damage accumulation from edge notches into the specimen interior occurs under T-C fatigue. Resistance to damage accumulation under T-C cycling can be effectively compared for various laminates by measuring changes in Δ(COD) during cycling. A critical Δ(COD) exists for failure.

References

[1] Chang, F. H. *et al.* in *Composite Reliability*, ASTM STP 580, 1975, pp. 176-189.

[2] Ramani, S. V. and Williams, D. P. in *Failure Modes in Composites III*, 1976, The Metallurgical Society of AIME, 345 East 47th Street, N.Y.

[3] Hahn, H. T. and Awerbuch, J. in *Mechanics of Composites Review*, Dayton, Ohio, 1976.

[4] Ryder, J. T. in *Mechanics of Composites Review*, Dayton, Ohio, 1976.

[5] Pagano, N. J. and Pipes, R. B., *International Journal of Mechanical Sciences*, Vol. 15, No. 8, 1973, pp. 679-688.

[6] Crossman, F. W., Lockheed Palo Alto Research Laboratory Report, LMSC/D084423, 1976, LPARL, Palo Alto, Calif.

[7] Sendeckyj, G. P. in *Failure Modes in Composites III*, 1976, The Metallurgical Society of AIME, 345 East 47th Street, N.Y.

TABLE 1 — *Static strengths of the laminates.*

Laminate	Unnotched Strength, MN/m^2	Notched Strength (σ_{gross}, MN/m^2) (Average of 3 Specimens)		
		25 mm wide 3-mm DEN	50 mm wide 6-mm DEN	25 mm wide 3-mm CCN
$[0/\pm30]_{3s}$ AS/3501	850 ± 55 (20[a])	T[b] - 185[c] C[b] - 270[c]		
$[0/\pm30/0]_{2s}$ AS/3501	940 ± 100 (12)	T - 270	T - 235 C - 220	
$[0/\pm45/0]_{2s}$ AS/3501	725 ± 140 (16)	T - 240 C - 350	T - 150[d] C - 215[d]	
$[0/\pm45/0]_{2s}$ T300/934	850 ± 35 (12)		T - 310 C - 220	T - 440
$[0/\pm45/90]_{2s}$ T300/934	550 ± 30 (12)		T - 235 C - 220	T - 325

[a] Number of specimens tested.

[b] T = tension, C = compression.

[c] 6-mm DEN.

[d] 10-mm DEN.

TABLE 2 — *Rate of damage accumulation under T-C cycling for the* $[0/\pm30]_{3s}$ *laminate.*

Spec. No.	$\Delta\sigma$, MN/m^2	% Life Spent in Stage I	Stage I[b] Slope (m), mm/Cycle	Stage II[c] Slope (m'), $Cycle^{-1}$	N_f, Cycles to Failure
1	538 (207,331)[a]	88	5×10^{-8}	1.5×10^{-5}	1.2×10^{6}
2	572 (241,331)	77	1.3×10^{-7}	7.1×10^{-5}	4×10^{5}
3	627 (241,386)	66	9.8×10^{-7}	3.3×10^{-4}	4×10^{4}

[a] Tension, compression.

[b] $\Delta COD = mN + constant$.

[c] $\frac{d(\Delta COD)}{dN} = m'(\Delta COD) - constant$.

TABLE 3 — *Rate of damage accumulation in T-C fatigue for the* $[0/\pm\theta/0]_{2s}$ *(*θ *= 30°, 45°) and* $[0/\pm45/90]_{2s}$ *laminates (50 mm wide, 6-mm DEN plate specimens).*

Laminate	Spec. No.	$\Delta\sigma$, MN/m^2	Stage I[a] Slope (m), mm/Cycle	% Life Spent in Stage I	N_f, Cycles to Failure
$[0/\pm30/0]_{2s}$ AS/3501	1	425	2.1×10^{-7}	90	1.9×10^{5}
	2	425	2.3×10^{-7}	85	1.2×10^{5}
	3	405	1.3×10^{-8}	100	$3\times10^{6}\rightarrow$[b]
$[0/\pm45/0]_{2s}$ AS/3501	1	400	1×10^{-7}	75	8.3×10^{5}
	2	380	2.4×10^{-9}	100	$5\times10^{6}\rightarrow$
$[0/\pm45/0]_{2s}$ T300/934	1	460	4.9×10^{-9}	90	3.2×10^{6}
$[0/\pm45/90]_{2s}$ T300/934	1	360	2.4×10^{-8}	--	1.6×10^{6}

[a] $\Delta COD = mN + constant$.

[b] $\rightarrow$ = run-out specimen.

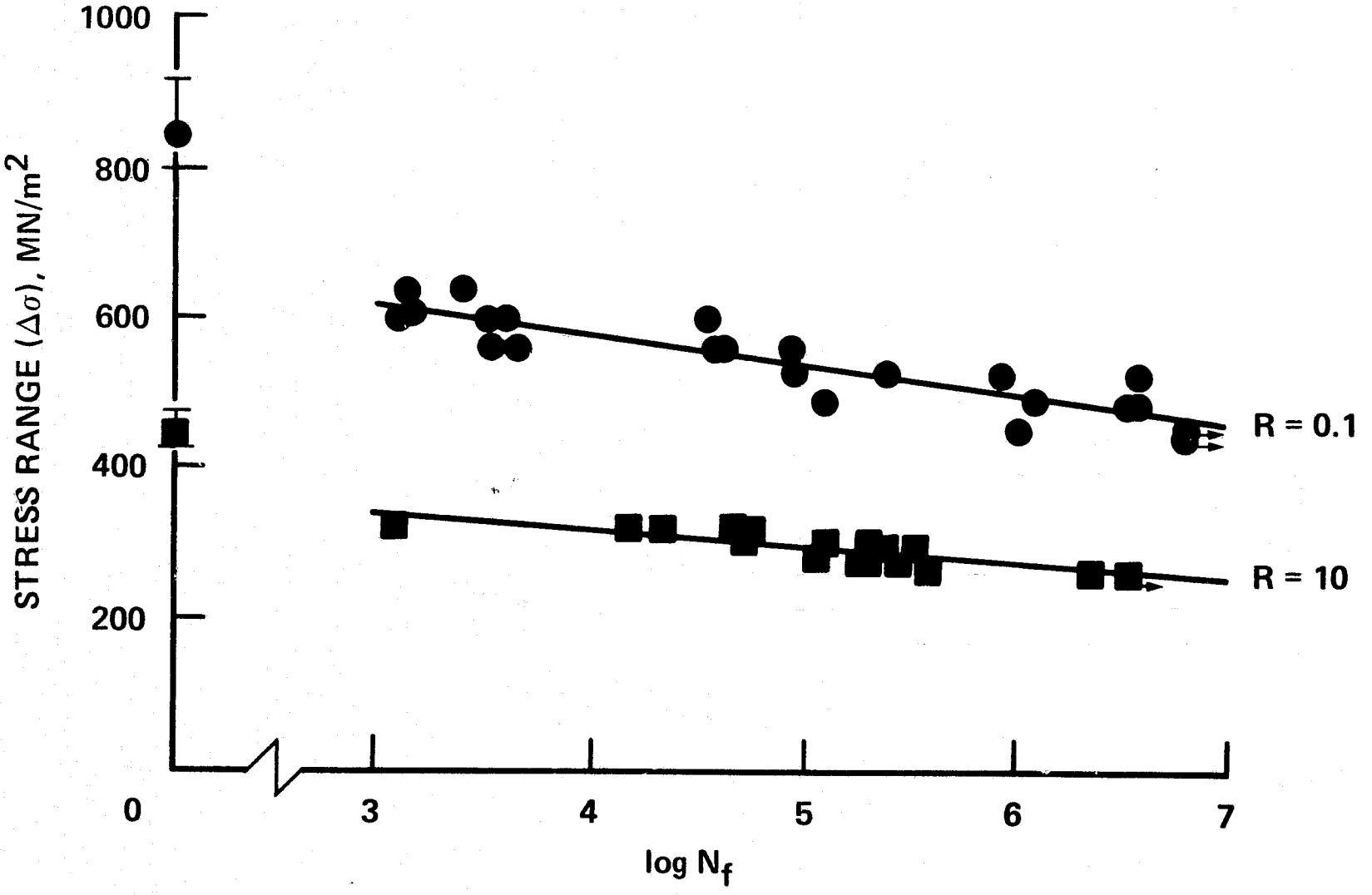

FIG. 1— S-N curves of $[0/\pm30]_{3s}$ graphite/epoxy.

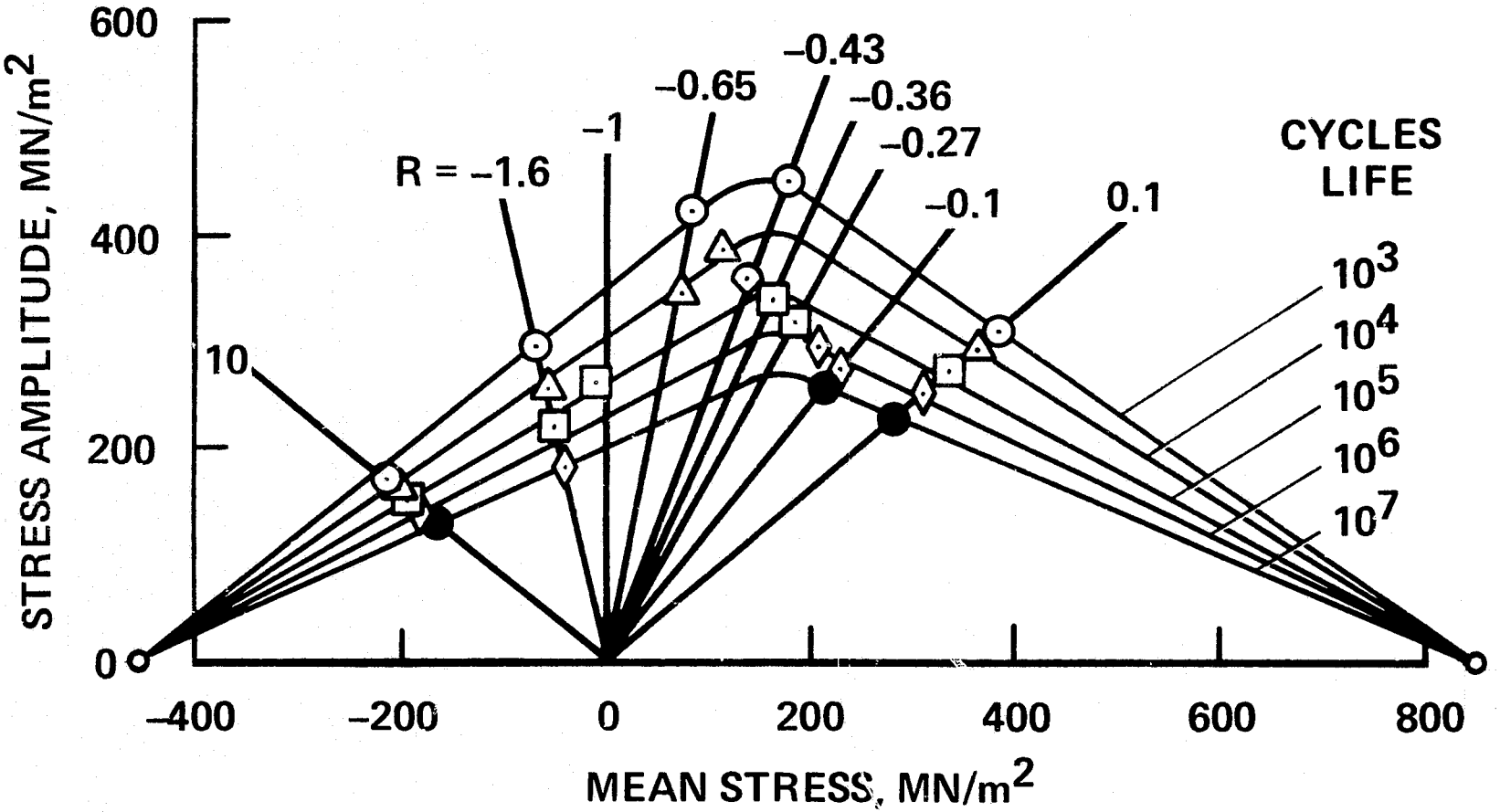

FIG. 2— Goodman Diagram for $[0/\pm30]_{3s}$ graphite/epoxy.

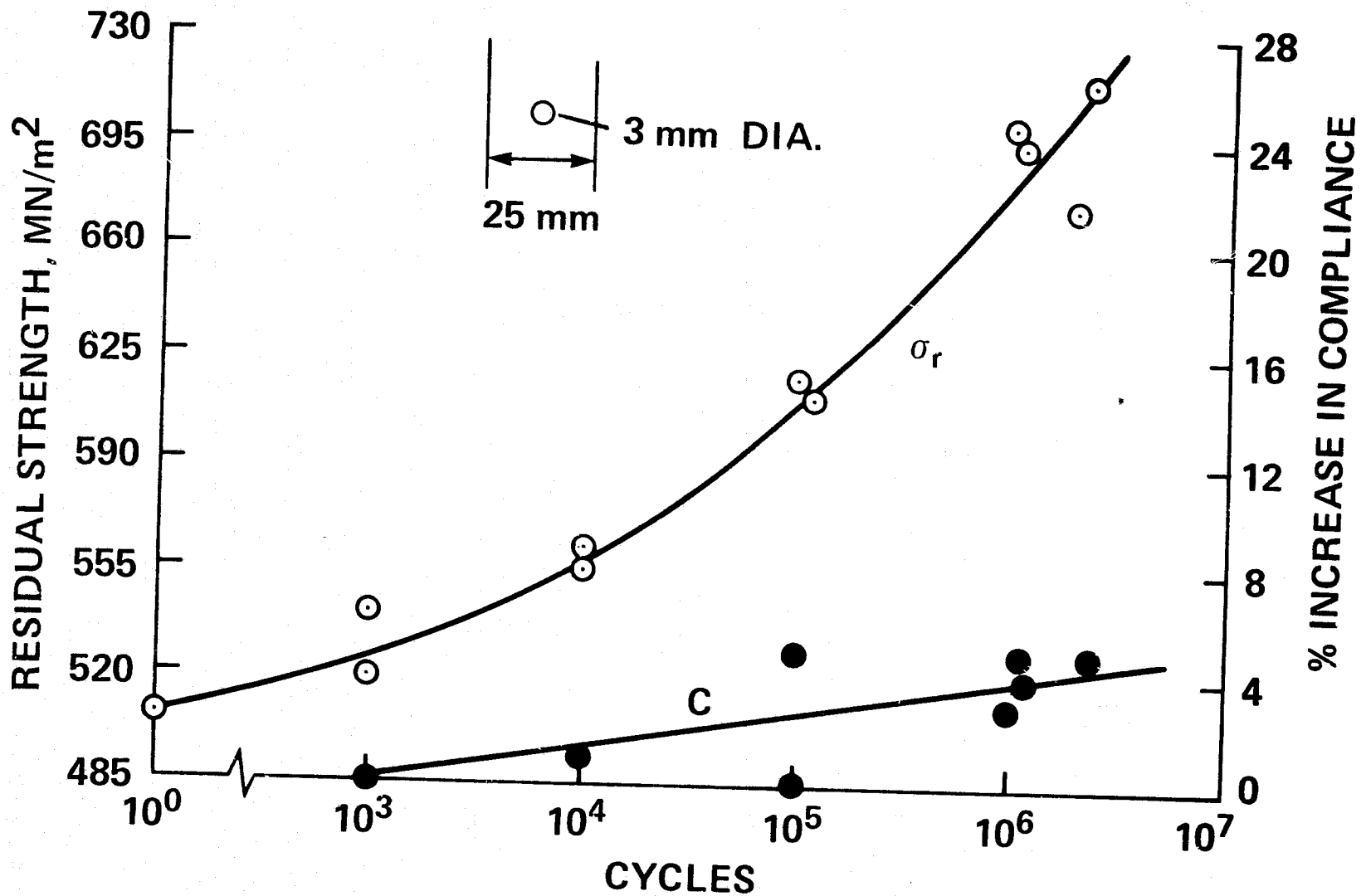

FIG. 3— Changes in residual strength and compliance for notched $[0/\pm45/0]_{2s}$ T300/934 laminate cycled in T-T.

FIG. 4— X-ray radiographs of damage accumulation in notched $[0/\pm45/0]_{2s}$ T300/934 laminate subjected to T-T fatigue.

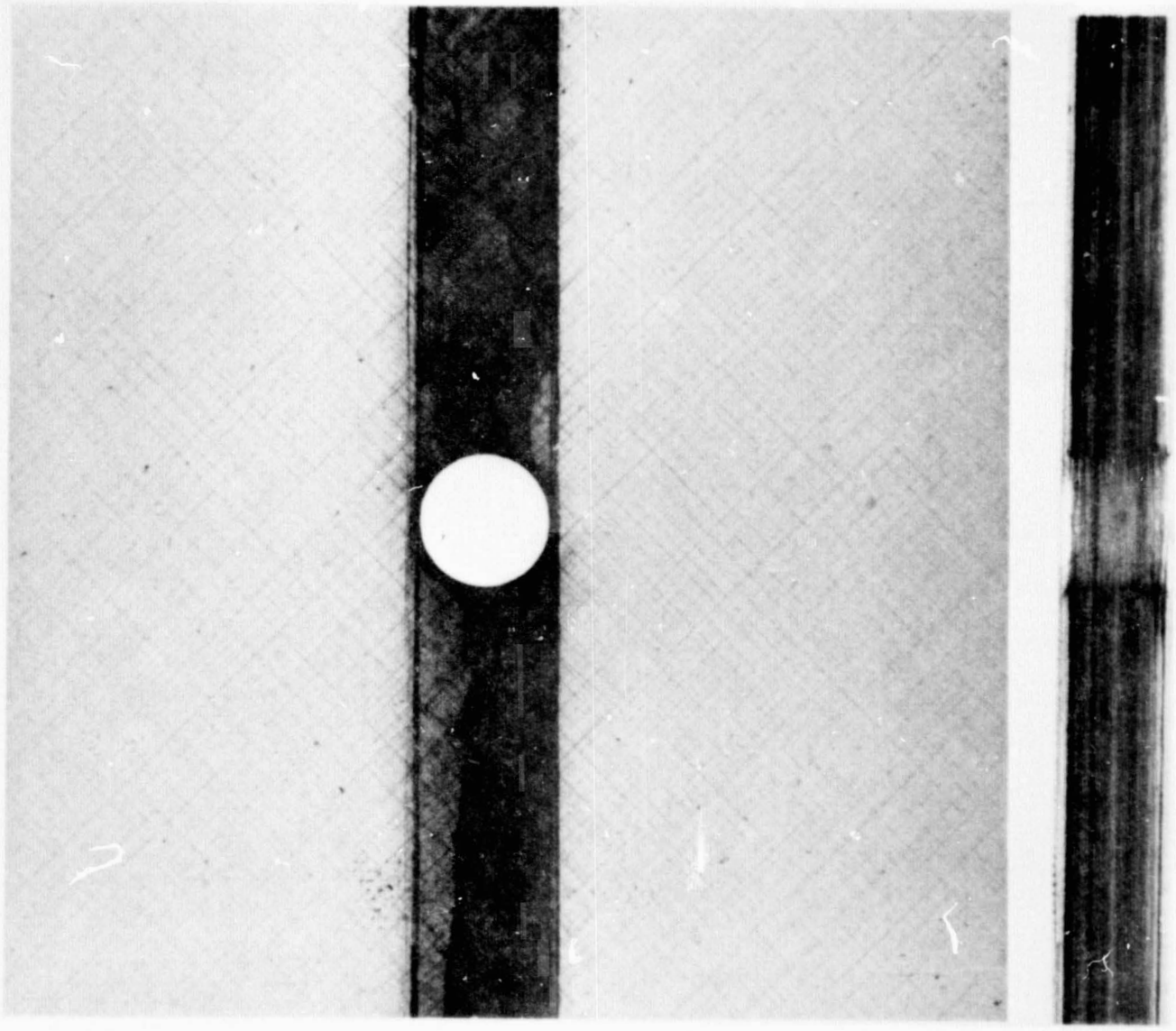

FIG. 5— X-ray radiograph of damage in notched $[0/\pm45/0]_{2s}$ T3-0/934 laminate after 3×10^6 cycles at $\Delta\sigma = 0.7\,\sigma_u$.

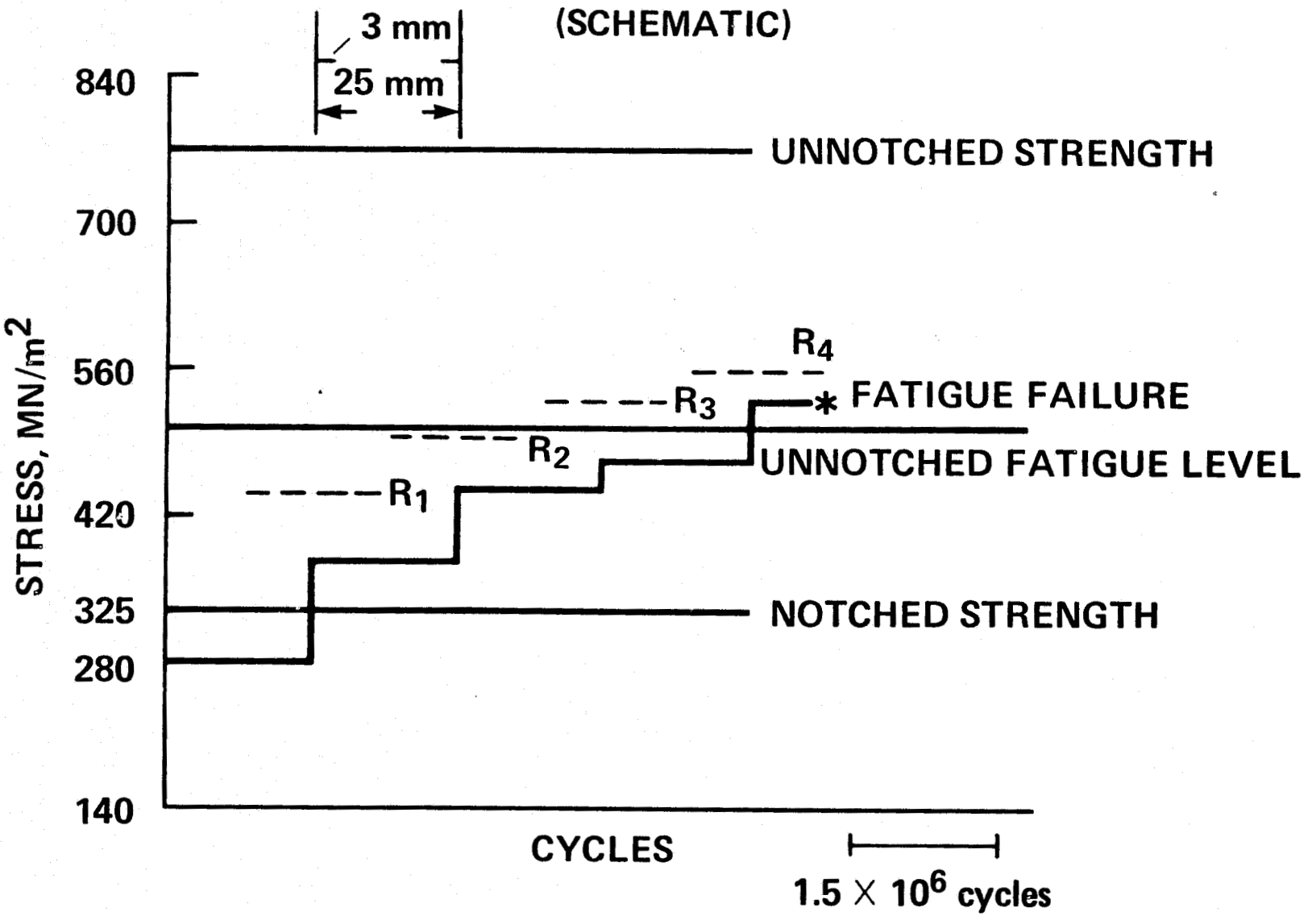

FIG. 6— Schematic illustration of fatigue failure of edge-notched $[0/\pm45/0]_{2S}$ AS/3501 laminate in T-T.

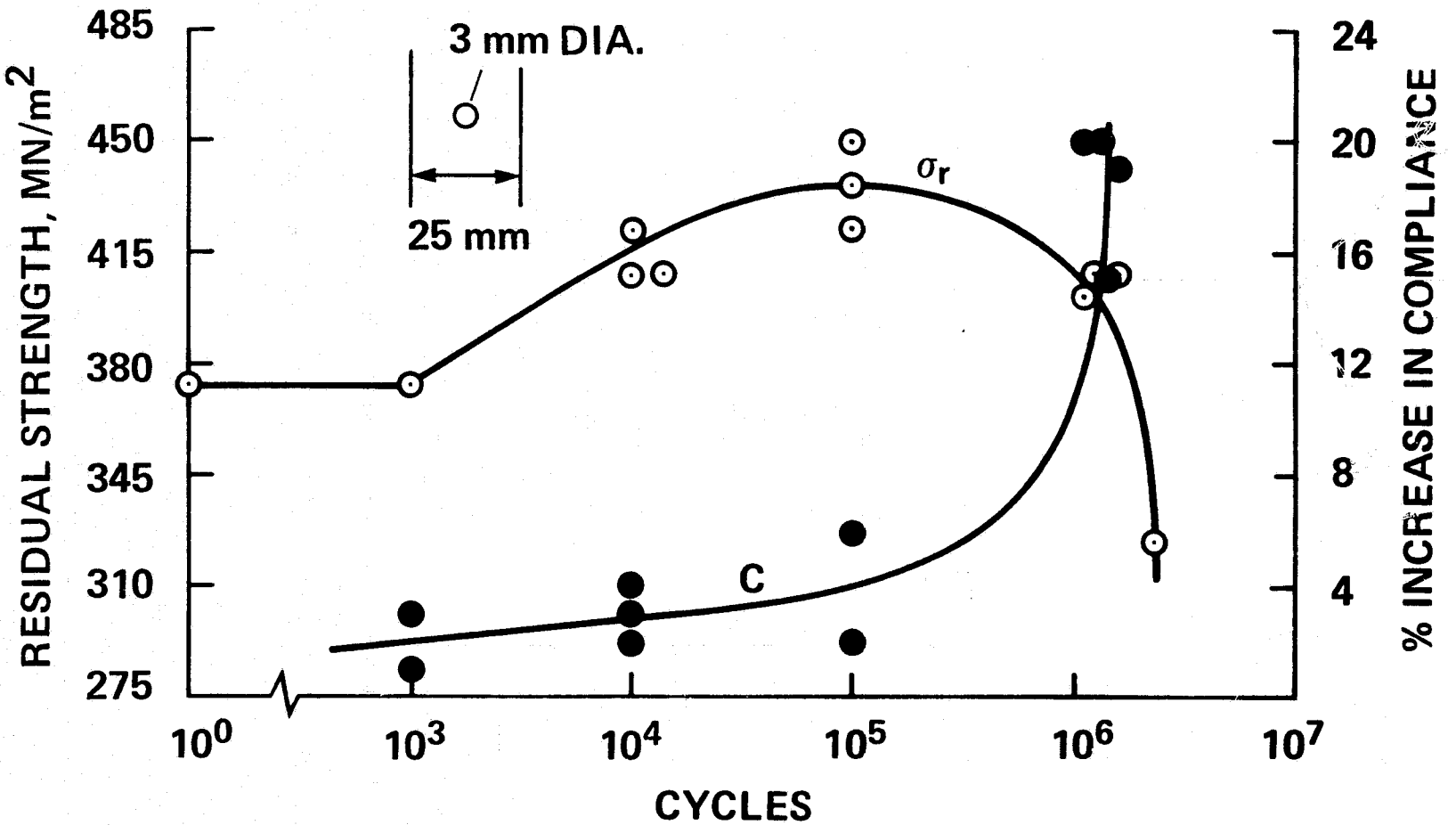

FIG. 7— Changes in residual strength and compliance for notched $[0/\pm45/90]_{2s}$ T300/934 laminate cycled in T-T.

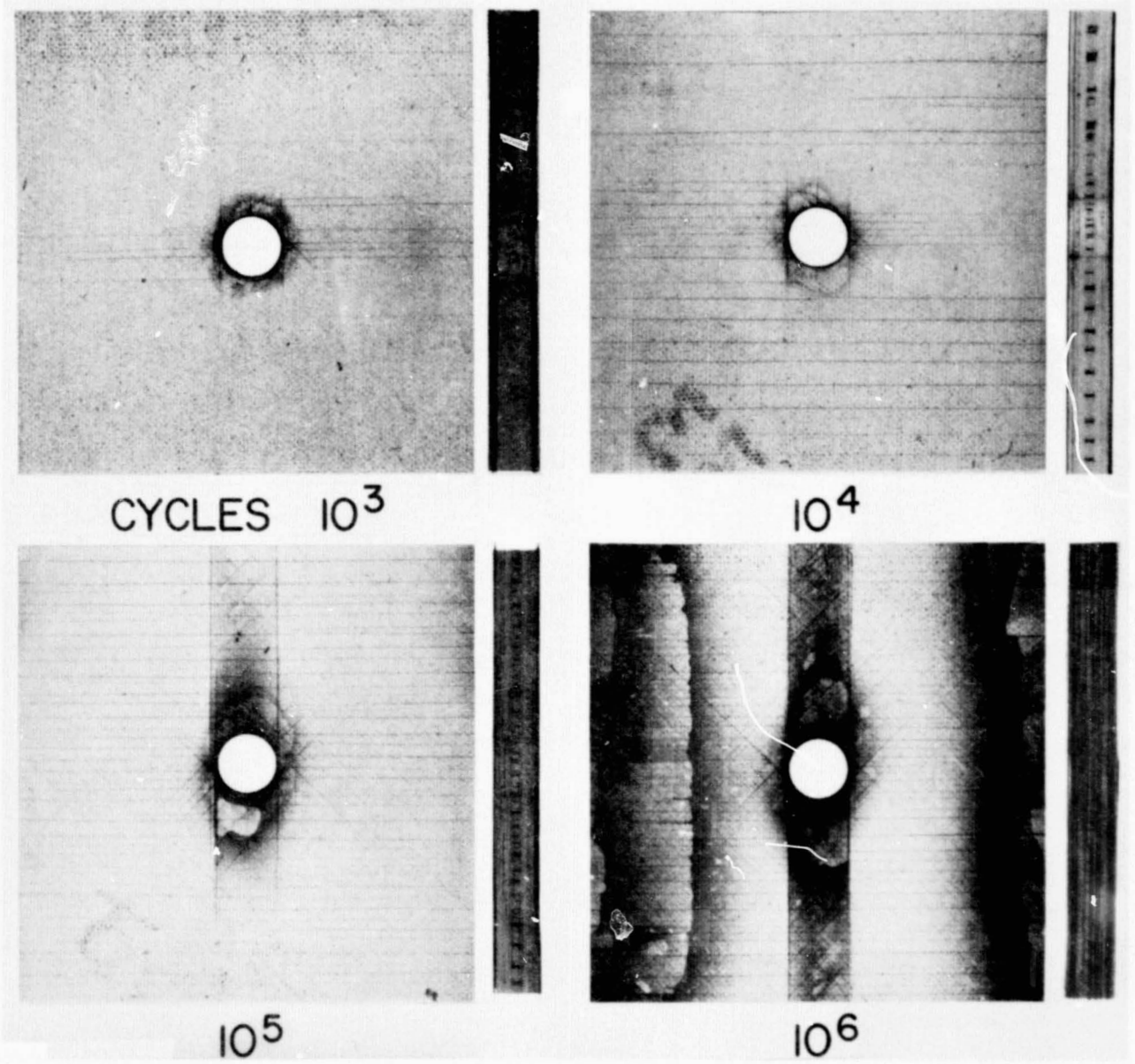

FIG. 8— X-ray radiographs of damage accumulation in notched $[0/\pm45/90]_{2s}$ T300/934 laminate subjected to T-T fatigue.

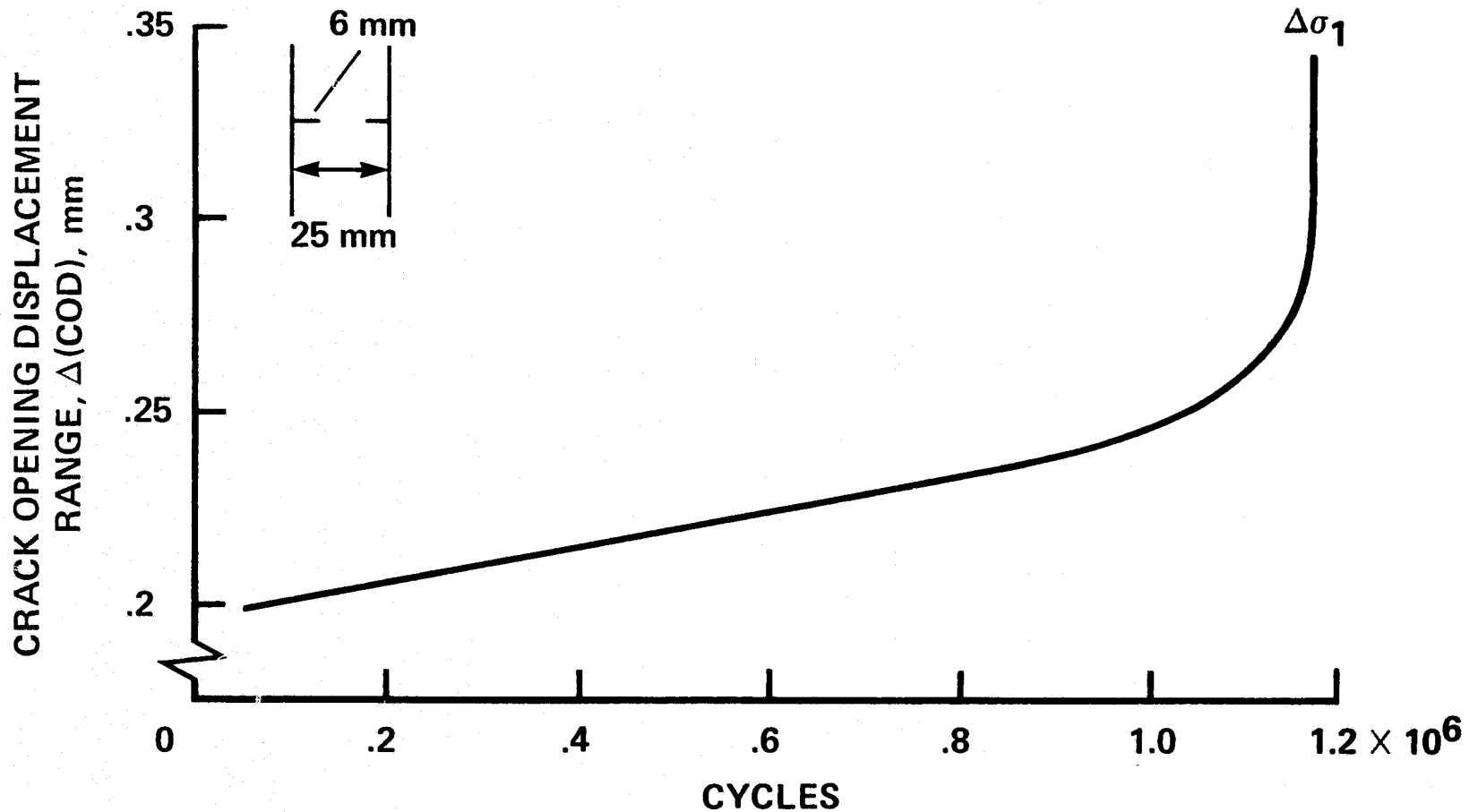

FIG. 9— Typical damage accumulation curve for the $[0/\pm30]_{3s}$ laminate under T-C cycling.

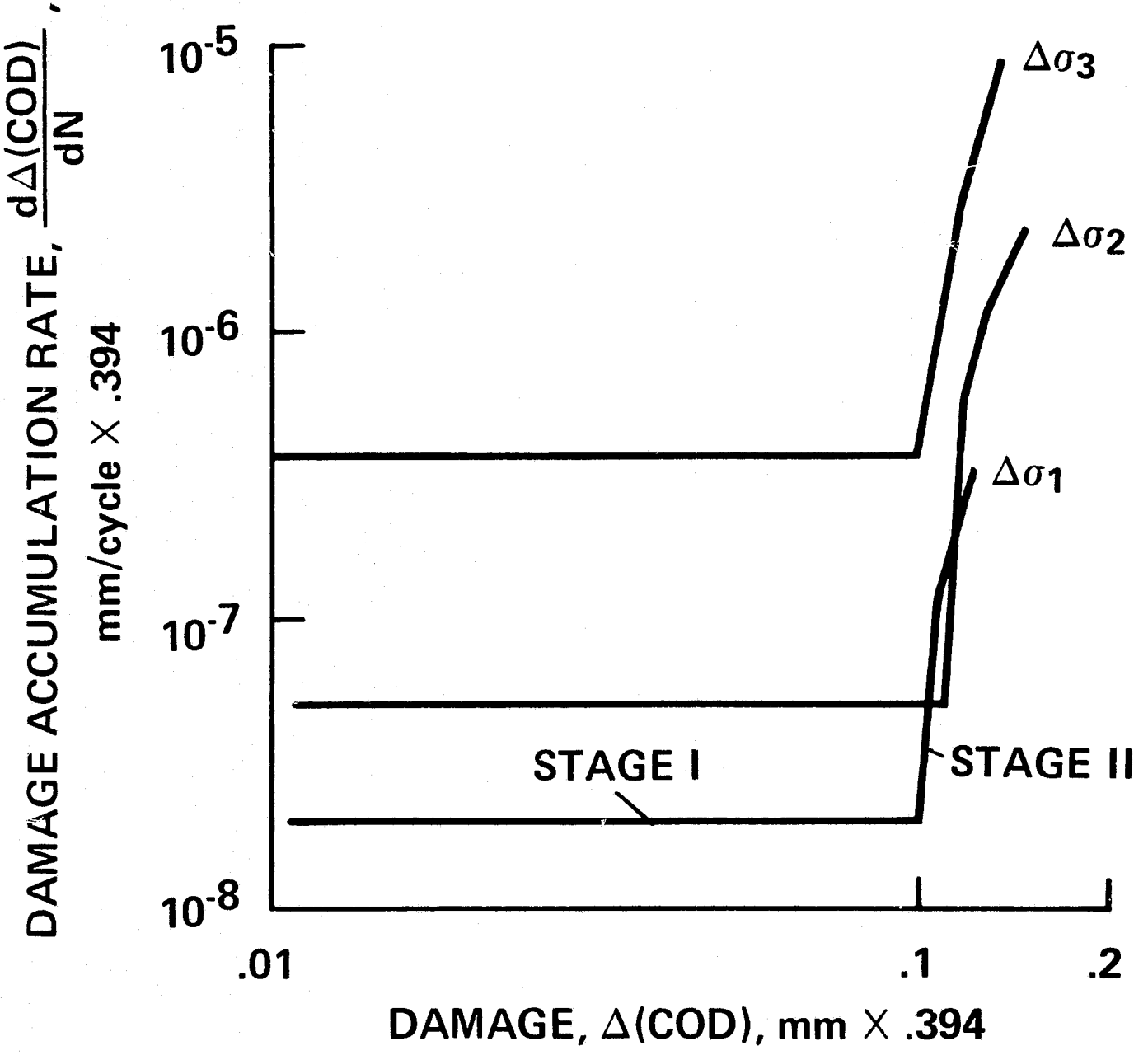

FIG. 10— Rate of damage accumulation versus damage curves for the $[0/\pm30]_{3s}$ laminate at three cyclic stress ranges in T-C fatigue.

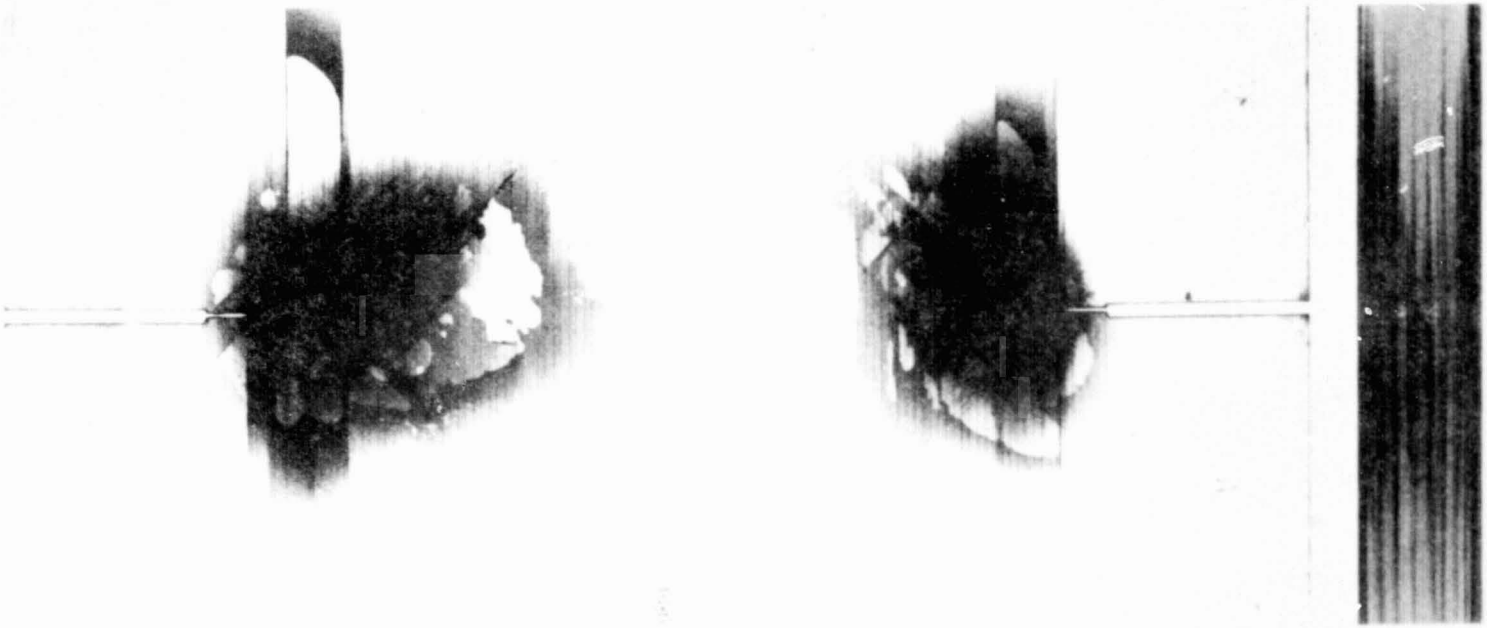

FIG. 11— X-ray radiograph of damage buildup under T-C cycling in notched $[0/\pm45/0]_{2s}$ laminate near failure (~10^6 cycles).